HgCdTe ENERGY GAP DETERMINATION FROM PHOTOLUMINESCENCE AND SPECTRAL RESPONSE MEASUREMENTS

Krzysztof Murawski, Małgorzata Kopytko, Paweł Madejczyk, Kinga Majkowycz, Piotr Martyniuk

Military University of Technology, Institute of Applied Physics, 2 Kaliskiego St., 00-908 Warsaw, Poland
(✉ *krzysztof.murawski01@wat.edu.pl, malgorzata.kopytko@wat.edu.pl, pawel.madejczyk@wat.edu.pl, kinga.majkowycz@wat.edu.pl, piotr.martyniuk@wat.edu.pl*)

Abstract

The temperature dependence of photoluminescence spectra has been studied for the HgCdTe epilayer. At low temperatures, the signal has plenty of band-tail states and shallow/deep defects which makes it difficult to evaluate the material bandgap. In most of the published reports, the photoluminescence spectrum containing multiple peaks is analyzed using a Gaussian fit to a particular peak. However, the determination of the peak position deviates from the energy gap value. Consequently, it may seem that a blue shift with increasing temperature becomes apparent. In our approach, the main peak was fitted with the expression proportional to the product of the joint density of states and the Boltzmann distribution function. The energy gap determined on this basis coincides in the entire temperature range with the theoretical Hansen dependence for the assumed Cd molar composition of the active layer. In addition, the result coincides well with the bandgap energy determined on the basis of the cut-off wavelength at which the detector response drops to 50% of the peak value.

Keywords: infrared detectors, HgCdTe, photoluminescence, spectral responsivity, semiconductor energy gap.

1. Introduction

Detectors operating in the *mid-wave infrared* (MWIR) (3–5 μm) and *long-wave infrared* (LWIR) (8–14 μm) range are used in many industries and science, which is related to the absorption spectrum of the atmosphere. Despite the development of competing technologies [1], mercury-cadmium telluride ($Hg_{1-x}Cd_xTe$) is still the basic semiconductor for *infrared* (IR) detectors in this spectral range [2]. Although this material has been studied since the 1960s, the determination of the energy gap (E_g) from experimental data is not described unequivocally in the literature. This material shows the dependence of the band gap energy on temperature T and Cd molar composition x. Correct determination of the semiconductor energy gap is necessary for

scientists designing IR devices and performing their numerical analyses. Several expressions on T and x dependences of the HgCdTe energy gap have been presented in the literature [3–6], and the most commonly used is the empirical expression reported by Hansen *et al.* [7].

$$E_g(x,T) = -0.302 + 1.93x - 0.81x^2 + 0.832x^3 + 5.35 \times 10^{-4}(1 - 2x)T. \tag{1}$$

It was developed on the basis of a variety of literature sources covering the ranges over $0 < x <$ and 4.2 K $< T < 300$ K. The data used in the fitting of this expression were obtained from optical absorption and magneto-optical experiments.

Apart from the Cd molar composition and temperature, the influence of defects, naturally present in a certain density in narrow-bandgap HgCdTe, should also be highly considered during the experiment. *Photoluminescence* (PL) is the key technique to investigate the *band-to-band* (BtB), as well as defect-related transition in small-compositional HgCdTe, however, it causes difficulties in the evaluation of the material bandgap. The relaxation process greatly favors low-energy states, resulting in a significant PL signal and leading to a broadening of the PL spectra at low temperatures. In addition, due to the narrow bandgap, the PL signal is affected by other phenomena such as the free carrier emission, which in turn may overestimate the E_g value at high temperatures. Moreover, one should pay attention to what theory is used to analyze the PL signal. In most of the published reports, a PL spectrum containing multiple peaks is analyzed using a Gaussian fit to a particular peak [8–11]. However, it should then be assumed that the carrier distribution function obeys the Boltzmann statistics, and the energy of electron density maximum is related to the ideal material bandgap by a factor of $k_B T/2$ for momentum non-conserving transitions, where k_B is the Boltzmann constant and T is temperature. For momentum non-conserving transitions, the shift of the PL peak with respect to the E_g is equal to $2k_B T$. If one estimates E_g from the PL peak maximum, the results deviate from the theoretical Hansen's relation [11]. While the difference is not significant at low temperatures, at high temperatures this inaccuracy increases. The determination of the energy gap from the PL measurements is rather difficult also in III-V materials, including *type II superlattices* (T2SLs), where the PL peak energy exhibits S-shape-like behavior – it is red-shifted at low temperatures due to the carrier localization and blue-shifted at high temperatures due to the free carrier emission [12]. In this case, *photoreflectance* seems to be the better method (PR) as it is able to probe excited states and small oscillator strength transitions. PR is especially useful in analyzing optical transitions in low-dimensional structures, such as quantum wells (QWs) [13–16].

Another method commonly used to determine the energy gap of a semiconductor is measuring the *spectral response* (SR) of the detector. In general, E_g can be safely associated with the wavelength corresponding to the half-peak response value, *i.e.* where the SR signal drops to 50% of the peak value [17–19]. The exponential part of the SR for wavelengths greater than the cut-off wavelength (less than 50% of the detector response) is related to the Urbach tail. Such assumption is found in most of literature reports and is valid when the spectral roll-off is reasonably sharp. However, it is not exact for LWIR detectors for which the spectral roll-off is rather soft due to the fact that the penetration depth of the radiation is much greater than the thickness of the absorbers used. The radiation losses due to too thin an absorber cause a drop in the *quantum efficiency* (QE). Then, the use of the half-peak response value criteria overestimates the E_g value. In such cases, other cut-off wavelength criteria are used, *e.g.* for 10% of the peak response value or at the point of intersection of the tangent to the SR edge with the horizontal axis [20]. The latter method, however, causes an underestimation of the E_g when the Urbach tail is observed [21].

When determining the bandgap energy of a semiconductor, especially in the case of a narrow bandgap semiconductor material with a large number of dopants and impurities, several independent measurement methods should be used. In this paper, on the example of an MWIR HgCdTe

heterostructure photodiode, we show how to determine the temperature dependence of energy gap of the active layer using the two mentioned measurement methods. By comparing the PL and SR signals on one graph it is possible to determine which of the peaks visible on the PL spectrum came from the BtB transition. Then, analyzing the PL signal by a theoretical expression, which takes into account the Boltzmann distribution function, the E_g value can be determined. This approach gives the E_g temperature dependence in accordance with the theoretical Hansen's relation.

2. Theory of measurement methods

2.1. Responsivity

The SR of the photodetector is the wavelength range over which the detector is sensitive to incident optical radiation. It is conceptually similar to QE, which gives the number of electron-hole (e–h) pairs generated for every incoming photon. Ignoring the radiation reflection on the semiconductor surface, the QE of the photodetector is given by [22].

$$QE(\lambda) = 1 - \exp\left[-\alpha(\lambda) \cdot t\right], \tag{2}$$

where $\alpha(\lambda)$ is the absorption coefficient and t is the photodetector's active layer thickness. When all incident radiation is absorbed within the entire thickness of the absorber, the QE has an ideal square shape (Fig. 1a). Otherwise, radiation losses are observed as a reduction in the QE.

Unlike the square shape of the ideal QE, the SR decreases at small photon wavelengths, at which each photon has a high energy, according to the relation

$$SR(\lambda) = \frac{\lambda}{hc}QE(\lambda) = \frac{\lambda}{1.238}QE(\lambda), \tag{3}$$

where h is the Planck constant in [eV·s] and c is the velocity of light, and λ is the wavelength in [μm].

At long wavelengths, the SR is limited by the inability of the semiconductor to absorb photons with energies below the band gap, and the SR suddenly drops to zero. This limit is the same as for the QE curves and is called the cut-off wavelength, which is

$$\lambda_{\text{cut-off}} = hc/E_g = 1.238/E_g, \tag{4}$$

where $\lambda_{\text{cut-off}}$ is in [μm] and E_g is in [eV].

The Urbach tail is the exponential part in the SR for wavelengths larger than the cut-off wavelength and is included in the absorption coefficient.

2.2. Photoluminescence

PL is the emission of light from a semiconductor after the absorption of photons. The PL observation at a certain energy can be taken as an indication that an electron populated an excited state associated with this transition energy. A theoretical approach to solving this problem is given by the PL equations of semiconductors.

In ideal semiconductors, with no energy level within the band gap, electrons and holes recombine from the *conduction band* (CB) and *valence band* (VB) extremes, respectively. The energy of this transition is equal to the energy gap of the semiconductor. As presented in Fig. 1b,

www.czasopisma.pan.pl PAN www.journals.pan.pl

POLSKA AKADEMIA NAUK

K. Murawski et al.: HgCdTe ENERGY GAP DETERMINATION FROM PHOTOLUMINESCENCE...

the PL intensity of this transition is proportional to the product of joint density of states and the probability that the particle occupies a state with the energy E [23–25]

$$I_{PL}(E) = A\left(E - E_g\right)^n \exp\left(-\left(E - E_g\right)/k_B T\right), \tag{5}$$

where A is a scaling factor, and n is the parameter that can vary from 0.5 for the momentum conserving to 2 for momentum non-conserving transitions [23]. Figure 1 also shows exemplary values of the PL peak shift energy in relation to the bandgap energy, signed as ΔE, and the full-width-half-maximum (FWHM) of the PL spectrum.

To incorporate an Urbach tail for below-band-edge emission, the following equation should be used

$$I_{PL}\left(h\nu \leq E_{cr}\right) = AK \exp\left(\frac{\sigma}{k_B T}\left(E - E_{cr}\right)\right)$$
$$\times \exp\left(-\left(E - E_g\right)/k_B T\right), \tag{6}$$

where E_{cr} is the energy of the transition between Eqs. (3) and (4), K is a fixed parameter which ensures the smoothness of the transition, and σ describes the slope of the Urbach tail.
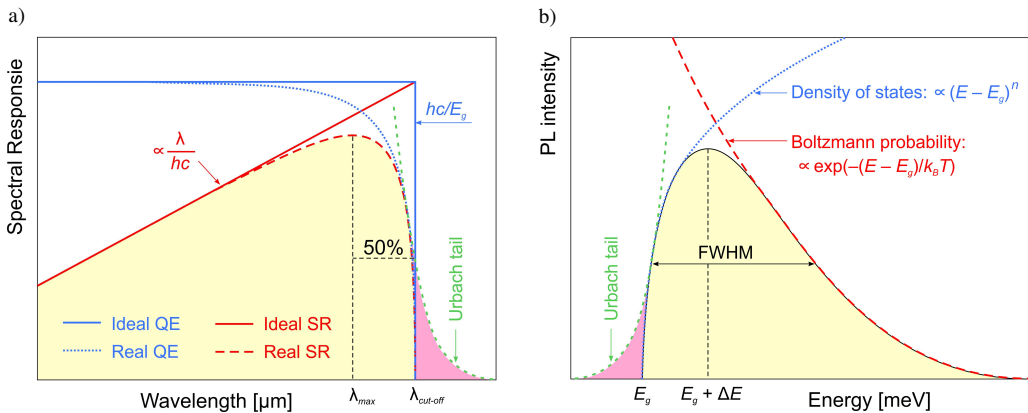

Fig. 1. Theoretical spectral response of photodiode (a) and photoluminescence spectra of a semiconductor epilayer (b).

3. Sample preparation and the measurement techniques

The analyzed HgCdTe epilayer was grown by a metal-organic chemical vapor deposition (MOCVD) on the GaAs substrate. The structure is back-side illuminated, so IR radiation incidences through the substrate which also makes it possible to produce an immersion lens that increases the detector's performance. Moreover, GaAs substrates are cheaper than, for example, CdZnTe, which reduces production costs. However, the crystal lattice mismatch between the GaAs substrate and the HgCdTe epitaxial layer requires the use of buffers – CdTe layers with a typical thickness of 3 μm. The final HgCdTe heterostructure consists of several layers: N+/p/T/P+/n+. At the very bottom is a heavily doped N+ contact layer with a composition of $x = 0.49$. The typical thickness is a few micrometers for low resistance, but for technological reasons associated with the etching it was extended to 10 μm. Next, there is the p-type absorber with a composition of $x = 0.29$ and an acceptor concentration assumed at the level of 4×10^{15} cm^{-3} to overcompensate

the donor-like background concentration. The thickness of the absorber is about 3 μm. The transient T layer is formed as a result of the specificity of MOCVD growth. It is the result of the diffusion of the next 1 μm thick P$^+$ layer with a composition significantly larger than that of the absorber and the acceptor concentration at the mid-10^{17} cm^{-3}. The n$^+$ layer with a composition lower than that of the absorber and donor concentration of about 10^{18} cm^{-3} is placed on top of the entire heterostructure to improve the electrical contact. 1 um thickness ensures low resistance.

For the SR measurements, a mesa structure detector was fabricated (Fig. 2a) using a standard processing procedure, including photolithography, wet chemical etching, metallization, cutting, and assembling. The SR characteristics were measured using a Perkin Elmer FT-IR spectrometer type Spectrum 2000. The detector was back-side illuminated and measured without biasing voltage. The absolute current responsivity values, in [A/W], were obtained by a measuring station composed of a lock-in analyzer, a monochromator, and a chopped 1,000 K blackbody. The SR characteristics were measured in the temperature range from 100 K to 300 K with the detector mounted in a liquid nitrogen cryostat.

For the PL measurements, the upper layers of the N$^+$/p/T/P$^+$/n$^+$ heterostructure were removed to collect the signal only from the active layer (see Fig. 2b). The successive n$^+$, P$^+$, and T layers were chemically etched and the p-type absorber layer was exposed. A 637 nm laser, mechanically chopped with a frequency of 100 Hz, was used as an excitation source. Measurements were made in the temperature range from 20 K to 300 K with a constant excitation power of 200 mW. The sample was in a helium cryostat with a temperature stabilization system. The PL signal was measured in the step-scan mode with a lock-in amplifier.
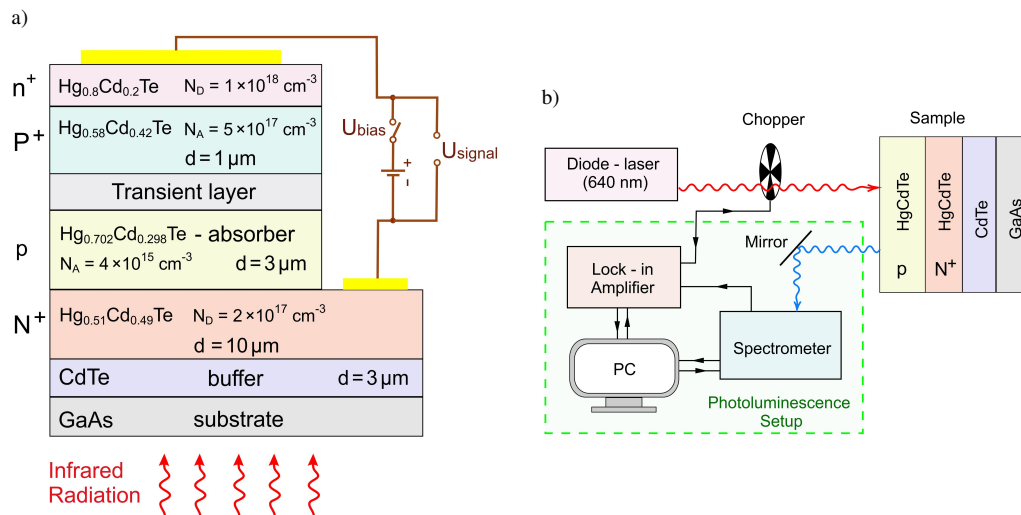

Fig. 2. MWIR N$^+$/p/T/P$^+$/n$^+$ HgCdTe heterostructure processed for spectral responsivity measurements (a) and photoluminescence measurement setup with an HgCdTe sample (b).

4. Determination of the temperature-dependent energy gap

The measured SR as a function of wavelength in the temperature range from 100 K to 300 K without biasing voltage for an HgCdTe heterostructure photodiode with the p-type HgCdTe absorber is shown on Fig. 3.
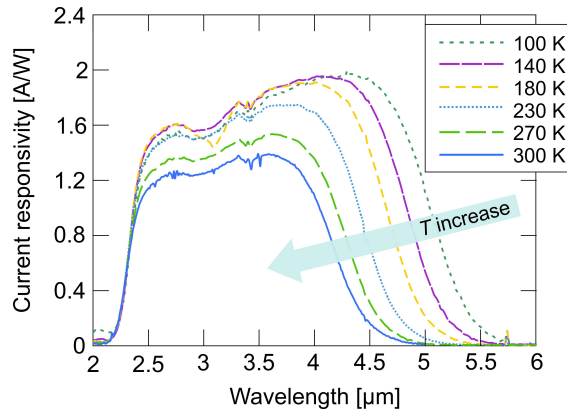
Fig. 3. Spectral characteristics of the MWIR N$^+$/p/T/P$^+$/n$^+$ HgCdTe heterostructure photodiode measured at various temperatures from 100 K to 300 K without biasing voltage.

At 230 K, the SR peak value is about 1.75 A/W at a wavelength of 3.8 µm. The cut-off wavelength of the detector is defined by the absorbers' composition. For the assumed value of $x = 0.298$, the $\lambda_{\text{cut-off}}$ at which the response drops to 50% of the peak value is equal to 4.4 µm at 230 K. In turn, the Cd composition of the N$^+$ layer determines the cut-on wavelength ($\lambda_{\text{cut-on}}$) of the detector. For the assumed value of $x = 0.49$, the $\lambda_{\text{cut-on}}$ at which the response increases to 50% of the peak value, is equal to 2.3 µm at 230 K. As can be seen in the case of HgCdTe, which is rarely found in semiconductor materials, the $\lambda_{\text{cut-off}}$ shifts towards shorter wavelengths as temperature increases, which means that the E_g value increases with increasing temperature.

Figure 4 shows the temperature-dependent PL measurements recorded in the range from 20 K to 300 K. At 20 K, the PL spectra are dominated by four peaks. Peak A has the highest PL intensity, which decreases and widens with increasing temperature. The relation of the peak A position and the energy gap calculation by using equation (5) exhibits that Peak A is due to the BtB passing. The Boltzmann factor in equation (5) determines the high-energy edge of the PL band, by which the fit to the shape of the A peak is particularly good at temperatures above 140 K. At low temperatures, Peak B with a larger energy than Phaneak A, is visible at the high-energy edge of Peak A. The PL Spectrum 4 also shows the transitions within the band gap, Peaks C and D, which make it difficult to determine the fundamental bandgap [26].

As mentioned above, in most of the published reports, a PL spectrum containing multiple peaks is analyzed applying a Gaussian fit to a particular peak. When we plot the PL peak versus temperature (see Fig. 5a), we can see that Peak A does not coincide with the theoretical Hansen's relation, but is at $E_g + k_B T/2$. Consequently, it may seem that a blue shift with increasing temperature becomes apparent. Thus, if one takes the correction for the $k_B T/2$ factor, as shown in Fig. 5b, Peak A corresponds well with the theoretical Hansen equation for $x = 0.298$, and also with the E_g value determined on the basis of equation (5).

Taking the position of the remaining peaks minus $k_B T/2$, it can be seen that the transitions for these peaks are parallelly shifted by a certain energy value with respect to the E_g. The transition energy of Peak B is of about 8 meV greater than the BtB transition (Peak A). The transition energy of the peaks C and D is of about 8 meV and 16 meV below the BtB transition, respectively. However, it should be noted that the nature of the remaining transitions was not the subject of this work.
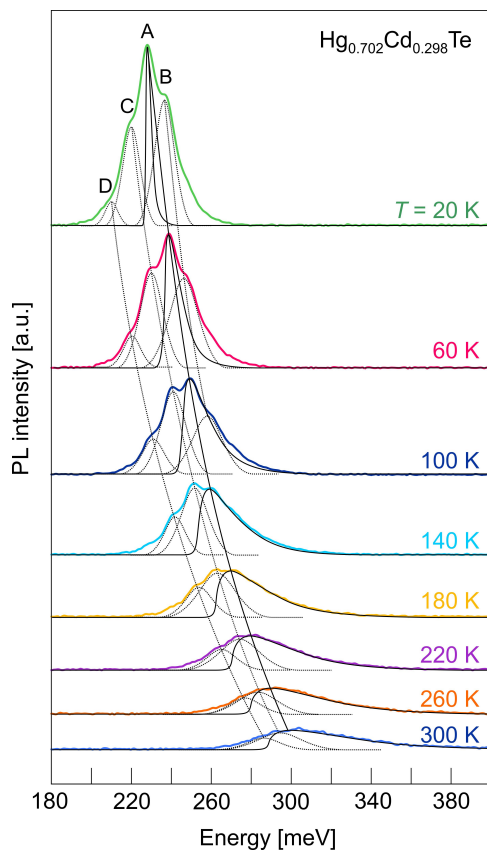
Fig. 4. Temperature-dependent PL spectra of an $Hg_{0.702}Cd_{0.298}Te$ epilayer
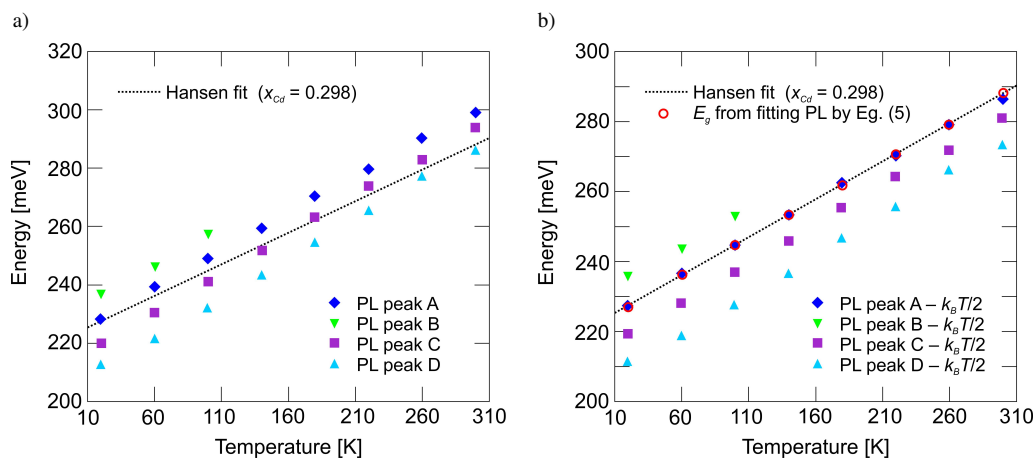measured in the range from 20 K to 300 K.

Fig. 5. Temperature dependence of the PL peak position (a) and the PL peak position with the correction for the $k_B T/2$
factor (b). The broken line is the HgCdTe bandgap calculated with the Hansen equation for $x = 0.298$. Red open circles
indicate the energy gap determined by equation (5).

189

5. Comparison of SR and PL signals

The determination of the fundamental bandgap has been confirmed by comparison of the photoluminescence and current responsivity spectra on one plot. Figure 6 shows the relative values of the PL and SR signals as a function of photon energy collected from the sample analyzed above at three temperatures. The PL peak which corresponds to the bandgap was fitted by equation (5). The E_g value determined on this basis coincides well with the energy determined on the basis of the cut-off wavelength at which the response drops to 50% of the peak value.
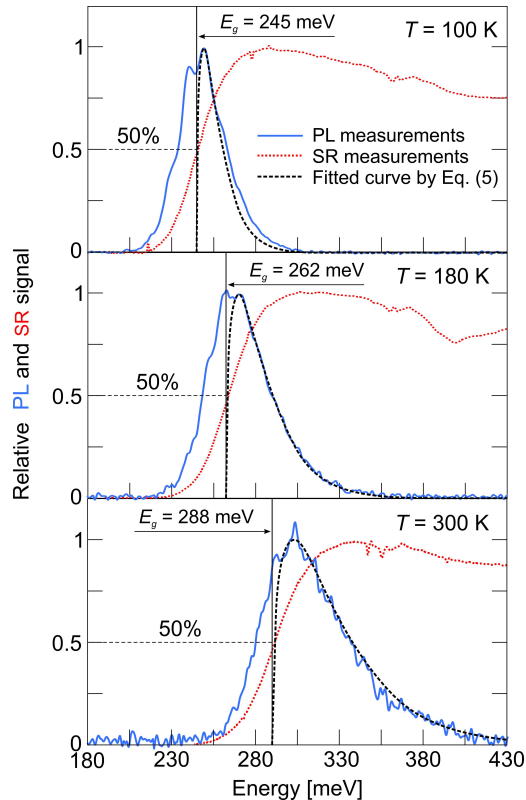

Fig. 6. Relative PL and SR signals as a function of the energy for an MWIR N⁺/p/T/P⁺/n⁺ HgCdTe heterostructure with Cd molar composition in the active layer of $x = 0.298$ measured at 100 K, 180 K, and 300 K. The broken line is the fit by equation (5) to the PL signal. Vertical lines indicate the energy gap determined by equation (5).

The comparison of the PL and SR signals was also performed for another HgCdTe sample. The design of the heterostructure is similar to that shown in Fig. 2, but the detector was optimized for a shorter wavelength range. The Cd molar composition in the active layer was assumed as $x = 0.305$. The results of the comparison collected at two temperatures are shown in Fig. 7. The PL spectrum has two visible peaks. By fitting the higher energy peak with equation (5), it can be seen that it is related to the BtB transition. The bandgap energy corresponds to the value for a half-peak of the SR signal. The low energy PL peak is contained in the Urbach tail on the SR of the detector.
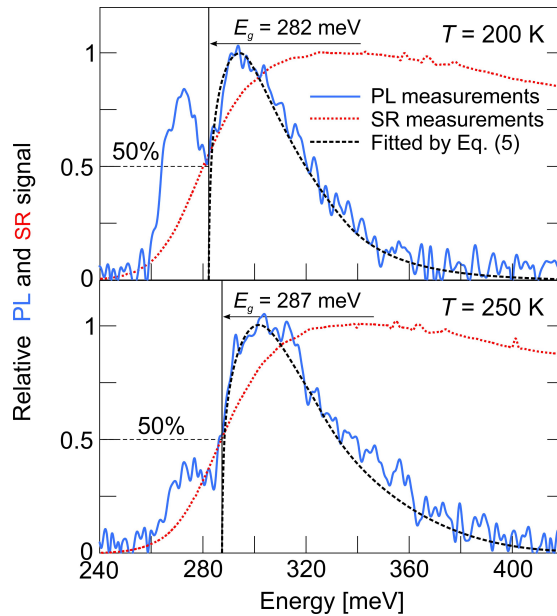
Fig. 7. Relative PL and SR signals as a function of the energy for an MWIR $N^+/p/T/P^+/n^+$ HgCdTe heterostructure with Cd molar composition in the active layer of $x = 0.305$ measured at 200 K and 250 K. The broken line is the fit by equation (5) to the PL signal. Vertical lines indicate the energy gap determined by equation (5).

6. Conclusions

Photoluminescence is a key technique to investigate optical transition in small-compositional HgCdTe, however, it causes difficulties in evaluation of the material bandgap when the signal is broadened. In the analyzed $N^+/p/T/P^+/n^+$ HgCdTe heterostructure, four active radial transitions are visible at low temperatures. To determine the energy gap of the active layer, the PL signal was fitted with the theoretical expression which is the product of joint density of states and the Boltzmann distribution function. This made it possible to determine the fundamental bandgap value, as opposed to fitting with the Gaussian function which overestimates the E_g by a factor of $k_B T/2$ when the PL peak position is determined. In order to distinguish the main transition from the others, the PL signal was compared with the spectral response of the detector. For different temperatures analyzed, the E_g value determined on from the PL measurements coincides well with the bandgap energy determined on the basis of the cut-off wavelength at which the detector response drops to 50% of the peak value. The E_g values are also consistent with the Hansen's formula for the assumed Cd molar composition of the active layer.

Acknowledgements

References

[1] Finkman, E., & Nemirovsky, Y. (1979). Infrared optical absorption of $Hg_{1−x}Cd_xTe$. *Journal of Applied Physics*, *50*(6), 4356–4361. https://doi.org/10.1063/1.326421

[2] Rogalski, A., Kopytko, M., Martyniuk, P., & Hu, W. (2020). Comparison of performance limits of HOT HgCdTe photodiodes with 2D material infrared photodetectors. *Opto-Electronics Review*, 82–92. https://doi.org/10.24425/opelre.2020.132504

[3] Schmit, J. L., & Stelzer, E. L. (1969). Temperature and Alloy Compositional Dependences of the Energy Gap of $Hg_{1−x}Cd_xTe$. *Journal of Applied Physics*, *40*(12), 4865–4869. https://doi.org/10.1063/1.1657304

[4] Wiley, J. D., & Dexter, R. N. (1969). Helicons and Nonresonant Cyclotron Absorption in Semiconductors. II. $Hg_{1−x}Cd_xTe$. *Physical Review*, *181*(3), 1181. https://doi.org/10.1103/PhysRev.181.1181

[5] Weiler, M. H. (1981). Defects, (HgCd) Se, (HgCd) Te. In R. K. Willardson, & A. C. Beer (Eds.), *Semiconductors and Semimetals*. Academic Press.

[6] Scott, M. W. (1969). Energy gap in $Hg_{1−x}Cd_xTe$ by optical absorption. *Journal of Applied Physics*, *40*(10), 4077–4081. https://doi.org/10.1063/1.1657147

[7] Hansen, G. L., & Schmit, J. L. (1982). Calculation of intrinsic carrier concentration in $Hg_{1−x}Cd_xTe$. *Journal of Applied Physics*, *54*(3), 1639–1640. https://doi.org/10.1063/1.330018

[8] Zhang, X., Shao, J., Chen, L., Lü, X., Guo, S., He, L., & Chu, J. (2011). Infrared photoluminescence of arsenic-doped HgCdTe in a wide temperature range of up to 290 K. *Journal of Applied Physics*, *110*(4), 043503. https://doi.org/10.1063/1.3622588

[9] Ivanov-Omskii, V. I., Mynbaev, K. D., Bazhenov, N. L., Smirnov, V. A., Mikhailov, N. N., Sidorov, G. Y., ... & Dvoretsky, S. A. (2010). Optical properties of molecular beam epitaxy-grown HgCdTe structures with potential wells. *Physica Status Solidi C, Current Topics in Solid State Physics*, *7*(6), 1621–1623. https://doi.org/10.1002/pssc.200983186

[10] Gemain, F., Robin, I. C., Brochen, S., Ballet, P., Gravrand, O., & Feuillet, G. (2013). Arsenic complexes optical signatures in As-doped HgCdTe. Applied Physics Letters, *102*(14), 142104. https://doi.org/10.1063/1.4801500

[11] Shao, J., Lu, W., Tsen, G. K. O., Guo, S., & Dell, J. M. (2012). Mechanisms of infrared photoluminescence in HgTe/HgCdTe superlattice. *Journal of Applied Physics*, *112*(6), 063512. https://doi.org/10.1063/1.4752869

[12] Steenbergen, E. H., Massengale, J. A., Ariyawansa, G., & Zhang, Y. H. (2016). Evidence of carrier localization in photoluminescence spectroscopy studies of mid-wavelength infrared InAs/InAs$_{1−x}$Sb$_x$ type-II superlattices. *Journal of Luminescence*, *178*, 451–456. https://doi.org/10.1016/j.jlumin.2016.06.020

[13] Shao, J., Yue, F., Lü, X., Lu, W., Huang, W., Li, Z., Guo, S. & Chu, J. (2006). Photomodulated infrared spectroscopy by a step-scan Fourier transform infrared spectrometer. *Applied Physics Letters*, *89*(18), 182121. https://doi.org/10.1063/1.2378675

[14] Shao, J., Chen, L., Lü, X., Lu, W., He, L., Guo, S., & Chu, J. (2009). Realization of photoreflectance spectroscopy in very-long wave infrared of up to 20 μ m. *Applied Physics Letters*, *95*(4), 041908. https://doi.org/10.1063/1.3193546

[15] Motyka, M., Sęk, G., Misiewicz, J., Bauer, A., Dallner, M., Höfling, S., & Forchel, A. (2009). Fourier transformed photoreflectance and photoluminescence of mid infrared GaSb-based type II quantum wells. *Applied Physics Express*, *2*(12), 126505. http://dx.doi.org/10.1143/APEX.2.126505

[16] Motyka, M., Sęk, G., Janiak, F., Misiewicz, J., Kłos, K., & Piotrowski, J. (2011). Fourier-transformed photoreflectance and fast differential reflectance of HgCdTe layers. The issues of spectral resolution and Fabry–Perot oscillations. *Measurement Science and Technology*, *22*(12), 125601. http://dx.doi.org/10.1088/0957-0233/22/12/125601

[17] Lin, C. T., Brown, G. J., Mitchel, W. C., Ahoujja, M., & Szmulowicz, F. (1998, April). Mid-infrared photodetectors based on the InAs/InGaSb type-II superlattices. In Photodetectors: Materials and Devices III (Vol. 3287, pp. 22–29). *SPIE*. https://doi.org/10.1117/12.304487

[18] Smith, E. P. G., Venzor, G. M., Petraitis, Y., Liguori, M. V., Levy, A. R., Rabkin, C. K., ... & Bangs, J. W. (2007). Fabrication and characterization of small unit-cell molecular beam epitaxy grown HgCdTe-on-Si mid-wavelength infrared detectors. *Journal of Electronic Materials*, *36*(8), 1045–1051. https://doi.org/10.1007/s11664-007-0169-6

[19] Hougen, C. A. (1989). Model for infrared absorption and transmission of liquid-phase epitaxy HgCdTe. *Journal of Applied Physics*, *66*(8), 3763–3766. https://doi.org/10.1063/1.344038

[20] Plis, E., Annamalai, S., Posani, K. T., Lee, S. J., & Krishna, S. (2006, May). Room temperature operation of InAs/GaSb SLS infrared photovoltaic detectors with cut-off wavelength ~5 μm. In Infrared Technology and Applications XXXII (Vol. 6206, pp. 225–233). *SPIE*. https://doi.org/10.1117/12.669172

[21] Martienssen, W. (1957). Über die excitonenbanden der alkalihalogenidkristalle. *Journal of Physics and Chemistry of Solids*, *2*(4), 257–267. https://doi.org/10.1103/PhysRev.92.1324

[22] Rogalski, A. (2010). *Infrared Detectors* (2nd ed.). CRC Press.

[23] Fang, Z. M., Ma, K. Y., Jaw, D. H., Cohen, R. M., & Stringfellow, G. B. (1990). Photoluminescence of InSb, InAs, and InAsSb grown by organometallic vapor phase epitaxy. *Journal of Applied Physics*, *67*(11), 7034–7039. https://doi.org/10.1063/1.345050

[24] Merrick, M., Cripps, S. A., Murdin, B. N., Hosea, T. J. C., Veal, T. D., McConville, C. F., & Hopkinson, M. (2007). Photoluminescence of InNAs alloys: S-shaped temperature dependence and conduction-band nonparabolicity. *Physical Review B*, *76*(7), 075209. https://doi.org/10.1103/76.075209

[25] Latkowska, M., Kudrawiec, R., Janiak, F., Motyka, M., Misiewicz, J., Zhuang, Q., ... & Walukiewicz, W. (2013). Temperature dependence of photoluminescence from InNAsSb layers: The role of localized and free carrier emission in determination of temperature dependence of energy gap. *Applied Physics Letters*, *102*(12), 122109. https://doi.org/10.1063/1.4798590

[26] Fuchs, F., & Koidi, P. (1991). Carrier localization in low-bandgap $Hg_{1-x}Cd_xTe$ crystals, studied by photoluminescence. *Semiconductor Science and Technology*, *6*(12C), C71. https://doi.org/10.1088/0268-1242/6/12C/013

Krzysztof Murawski is an assistant professor at the Institute of Applied Physics, Military University of Technology in Warsaw. He received his M.Sc. from the MUT in 2009 and his Ph.D. in material engineering in 2021 from the same university. The main subject of his research are AIIBVI-HgCdTe, AIIIBV InAsSb and T2SLs IR detectors.

Kinga Majkowycz is an engineer and PhD student at Institute of Applied Physics, Military University of Technology (MUT) in Warsaw. She received the M.Sc. degree in material engineering at the MUT in 2016. She is the author or co-author of reviewed journal papers and conference publications. She attended a six-month research internship in the VIGO Photonics in 2018 as well as a short research stay at the Faculty of Fundamental Problems of Technology, Wroclaw University of Science and Technology (2022). The main area of her research are technology of manufacturing IR detectors (AIIBVI-HgCdTe, AIIIBV InAsSb and T2SLs) and deep level transient spectroscopy.

Małgorzata Kopytko is an associate professor at the Institute of Applied Physics, Military University of Technology in Warsaw. She obtained her Ph.D. degree (2011) and D.Sc. degree (2018) in electronics from the Institute of Optoelectronics of thre same university. In her research she deals with narrow-bandgap semiconductor materials (HgCdTe, InAsSb, InAs/InAsSb superlattices) used for the design of uncooled infrared detectors.

Piotr Martyniuk Ph.D., Eng., is an associate professor at the Institute of Applied Physics, Military University of Technology (MUT) in Warsaw, Poland. He received the M.Sc. degree in technical physics from the MUT in 2001 and his Ph.D. in electronics from Warsaw University of Technology (2008). He has published over 170 reviewed journal papers and conference publications and co-authored one book: "Antimonide-based Infrared Detectors: A New Perspective". He cooperates with industry i.e. the VIGO Photonics within the joint MOCVD/MBE laboratory. In 2021 he was awarded with a 10 month Fulbright scholarship in OSU, KIND Laboratory in Ohio. His research focuses on $A^{II}B^{VI}$ and $A^{III}B^{V}$ based IR detectors.

Paweł Madejczyk received his M.Sc. degree in telecommunication from the Faculty of Electronics, Military University of Technology (MUT), Warsaw, in 1996. He joined the Institute of Applied Physics, MUT, in 1998 where he has investigated infrared detectors of mercury cadmium telluride (MCT). He received his Ph.D. degree in material engineering from the Faculty of Engineering, Chemistry and Technical Physics, MUT, in 2005. His current interests focus on higher operating temperature infrared detectors of metalorganic chemical vapor deposition (MOCVD) grown MCT heterostructures. He is the coauthor of more than 60 publications on infrared detectors and their applications.